

Published in final edited form as:

Clin Cancer Res. 2011 July 15; 17(14): 4751–4760. doi:10.1158/1078-0432.CCR-10-2098.

Prospective analysis of parametric MRI biomarkers: Identification of early and distinct glioma response patterns not predicted by standard radiographic assessment

Craig J. Galbán¹, Thomas L. Chenevert¹, Charles R. Meyer¹, Christina Tsien², Theodore S. Lawrence², Daniel A. Hamstra², Larry Junck³, Pia C. Sundgren¹, Timothy D. Johnson⁴, Stefanie Galbán², Judith S. Sebolt-Leopold¹, Alnawaz Rehemtulla^{1,2}, and Brian D. Ross¹

¹ Department of Radiology, University of Michigan, Center for Molecular Imaging, Ann Arbor, Michigan 48109 USA

² Department of Radiation Oncology, University of Michigan, Center for Molecular Imaging, Ann Arbor, Michigan 48109 USA

³ Department of Neurology University of Michigan, Center for Molecular Imaging, Ann Arbor, Michigan 48109 USA

⁴ Department of Biostatistics, University of Michigan, Center for Molecular Imaging, Ann Arbor, Michigan 48109 USA

Abstract

Purpose—Currently, radiologic response of brain tumors is assessed according to the Macdonald criteria 10 weeks from the start of therapy. There exists a critical need to identify non-responding patients early in the course of their therapy for consideration of alternative treatment strategies. Our study assessed the effectiveness of the Parametric Response Map (PRM) imaging biomarker to provide for an earlier measure of patient survival prediction.

Experimental Design—Forty-five high grade glioma patients received concurrent chemoradiation. Quantitative MRI including apparent diffusion coefficient (ADC) and relative cerebral blood volume (rCBV) maps were acquired pre-treatment and 3 weeks mid-treatment on a prospective institutional-approved study. PRM, a voxel-by-voxel image analysis method, was evaluated as an early prognostic biomarker of overall survival. Clinical and conventional MR parameters were also evaluated.

Results—Multivariate analysis showed that PRM_{ADC+} in combination with PRM_{rCBV} obtained at week 3 had a stronger correlation to one-year and overall survival rates than any baseline clinical or treatment response imaging metric. The composite biomarker identified three distinct patient groups, non-responders (median survival (MS) of 5.5 months CI: 4.4-6.6) months, partial responders (MS of 16 months CI: 8.6-23.4) and responders (MS has not yet been reached.)

Conclusions—Inclusion of PRM_{ADC+} and PRM_{rCBV} into a single imaging biomarker metric provided early identification of patients resistant to standard chemoradiation. In comparison to the current standard of assessment of response at 10 weeks (MacDonald Criteria) the composite PRM biomarker potentially provides a useful opportunity for clinicians to identify patients who may benefit from alternative treatment strategies.

Keywords

DW-MRI; DSC-MRI; glioma; prospective trial; treatment response

Introduction

The standard of care for patients with high grade gliomas is concomitant and adjuvant temozolomide and radiotherapy based on recent clinical results showing improved median and 5-year survival for patients treated with this chemoradiation regimen (1). Current clinical assessment of treatment response is determined 10 weeks post-treatment initiation based on Macdonald criteria(2-3). Limitations in accurate assessment of response has led to the development of a new standardized response criteria that accounts for transient changes in tumor volume post-therapy by the Response Assessment in Neuro-Oncology Working Group (RANO)(4). There exists a critical need for the development of individualized approaches to the treatment of this disease, which has a one year survival rate of roughly 50%. In this regard, *MGMT*-promoter methylation status is a potential predictive biomarker for selection of brain tumor patients who may derive the most benefit from treatment with temozolomide and radiotherapy (5). This initial success provides motivation for the development of non-invasive imaging biomarkers of response capable of predicting sensitivity to novel therapeutic interventions since not all patients are able to undergo surgical resection and provide sufficient tissue for *MGMT* analysis. The potential for using quantitative imaging modalities as early surrogate markers of response is compelling due to the ability to noninvasively detect treatment-associated functional and metabolic changes (6).

In this study, we investigated a multi-modality image-based response biomarker for high grade gliomas in order to more accurately predict treatment outcome early. Identification and validation of an image biomarker could provide the opportunity to select patients that may benefit from alternative treatment strategies. Quantitative magnetic resonance imaging (MRI) can provide structural and functional information regarding tumor cellularity and perfusion characteristics that compliment anatomical MRI. The value of this approach is that the microenvironment and physiology of the tumor can be monitored noninvasively, allowing for early assessment of tumor therapy response prior to treatment completion. Two techniques investigated for their diagnostic and prognostic value in brain tumor patients are diffusion weighted (DW)-MRI and dynamic susceptibility contrast (DSC)-MRI (7-8). DW-MRI, capable of measuring the random thermal (Brownian) motion of water, samples the tumor microenvironment on a subcellular level. A drop in tumor cellularity as a result of significant cell-kill following effective therapy has been associated with an increase in water diffusivity as expressed as the apparent diffusion coefficient (ADC) (9). This trend has been observed in preclinical and clinical studies supporting the notion of DW-MRI as a surrogate imaging biomarker for treatment response assessment in oncology (10-12). DSC-MRI, capable of quantifying changes in tumor hemodynamics, provides information on neovascularity and angiogenesis (13-17). At present, the relative cerebral blood volume (rCBV), as measured by DSC-MRI, has shown promise in determining tumor grade as well as prediction and early assessment of patient clinical response (18-21).

Imaging biomarkers (i.e. ADC or rCBV) of tumor response have historically been evaluated using the mean change in the whole tumor volume as the quantitative metric for detection of therapeutic efficacy. However, tumor heterogeneity is an inherent property of glioblastoma multiforme (GBM) and therefore standard methods of analysis using average values throughout an entire tumor can significantly under-estimate regional changes following therapy. In 2005 Moffat and colleagues proposed a new approach for evaluating tumor

response using serial ADC maps termed the “functional diffusion map” (fDM) (22). For the first time changes in ADC were evaluated on a voxel-wise basis by spatially aligning (via image registration) serial ADC maps acquired pre- and mid-therapy. The tumor volume fraction that exhibited a significant increase in mid-treatment ADC from baseline values was found to be predictive of 10 week radiological response in a cohort of 20 glioma patients as early as three weeks into therapy. This technique has now been established in multiple clinical sites, including breast cancer, prostate cancer, metastatic cancer to the bone and head and neck cancer (23-29). For the most part, this technique has only been applied to ADC maps. In 2009, the voxel-based approach was extended to rCBV maps acquired from DSC-MRI of 44 glioma patients. Now referred to more generally as the “parametric response map” (PRM), this post-processing approach when applied to rCBV (PRM_{rCBV}) was predictive of survival as early as one week post-treatment initiation as well as distinguishing progression from pseudo-progression (30-31).

We report here the outcome of a prospective single-center trial of WHO Gr 3 and 4 glioma patients that was designed to evaluate the predictive accuracy of PRM_{ADC} and PRM_{rCBV} imaging biomarkers as single and composite metrics of early treatment response as assessed 3 week post-treatment initiation. We compared parametric models using PRM imaging metrics from all patients (n=45) to assess correlation with one year and overall survival.

Results

Patient Population

A total of 45 subjects with high-grade glioma were included in this prospective study (Table 1). The median survival for the population, as determined by Kaplan-Meier analysis was 14.9 months (95% confidence interval: 8.6-21.2 months) with 56% of the patient population realizing one-year survival. Patients expiring prior to one year had a median survival of 6.6 months (95% confidence interval: 4.4-8.8 months) whereas those whose survival was beyond one year had a median survival of 35.1 months (95% confidence interval: 13.7-56.5 months). Patient age, Radiation Therapy Oncology Group Recursive Partitioning Analysis (RTOG RPA) (32) and Radiological Response (RR) at 10 weeks, were found to be significant predictors of one-year survival ($p=0.003$, $p=0.025$ and $p=0.001$, respectively) (Table 1).

Individually PRM_{ADC} and PRM_{rCBV} have been reported to be predictive biomarkers of clinical outcome (30, 33). The underlying mechanisms driving therapeutic-induced alterations in ADC and rCBV differ and therefore the predictive value of the outcome measures of PRM (PRM_{X+} and PRM_{X-}) vary on the quantitative parameter used for analysis. A large volume fraction of the tumor with significantly increasing ADC (PRM_{ADC+}) correlated with overall survival, unlike PRM_{ADC-} which had no predictive value. In stark contrast, a small volume fraction of tumor with decreasing rCBV (PRM_{rCBV-}) correlated with a positive outcome, where no predictive value was observed for PRM_{rCBV+} . Color-overlays of PRM_{ADC} and PRM_{rCBV} at week 3 post-treatment initiation of a representative responder (overall survival=17months; $PRM_{ADC+}=12\%$; $PRM_{rCBV-}=4\%$) and non-responder (overall survival=2months; $PRM_{ADC+}=1\%$; $PRM_{rCBV-}=40\%$) show spatial variation in the response of these tumors with respect to water diffusivity and blood volume (Figure 1). Both lesions had high vascular irregularities as can be presumed from the immense contrast-enhancement on the T1-weighted images (Figure 1A,D). The complex changes in tumor cellularity and vasculature following a therapeutic intervention appear from the PRM overlays to be somewhat dissociated from each other. For example, the responding tumor clearly showed regions of increased ADC, denoted in red, (Fig. 1B), which is associated with a loss in tumor cellularity. These same regions had statistically no change in rCBV (green area in Fig. 1E). In contrast, a significant volume of the non-

responding tumor showed no change in ADC, Figure 1C, suggesting no real loss of tumor cellularity. Unlike ADC, Figure 1F shows that a substantial fraction of tumor underwent a significant drop in rCBV post-treatment initiation, perhaps suggesting increased hypoxia in the tumor conferring radioresistance. Therefore, the combination of diffusion and perfusion imaging may provide complementary information that serves to improve sensitivity and specificity in predicting patient outcome. To evaluate a combined metric related to these physiological changes to treatment, we analyzed these parameters as a unified predictive metric of survival.

We first assessed the sensitivity of the individual parameter models (PRM_{ADC+} and PRM_{rCBV-}) and composite model (PRM_{ADC+/PRM_{rCBV-}}), as well as RR for comparison, to predict 6 month progression free survival (PFS) and one year survival in our cohort of patients using a logistic regression. Univariate analysis found a strong correlation of parametric models with both 6 month PFS and one year survival (Table 2). Inclusion of all four imaging metrics (PRM_{ADC+}, PRM_{rCBV-}, PRM_{ADC+/PRM_{rCBV-}} and RR) into a single multivariate logistic regression showed that PRM_{ADC+/PRM_{rCBV-}} and RR provided the strongest statistical power for assessing 6 month PFS ($p=0.012$ and $p=0.005$, respectively) but only PRM_{ADC+/PRM_{rCBV-}} for assessing one year survival ($p<0.0001$). To determine the statistical power of age, dichotomized based on responders ≥ 50 years and non-responders < 50 years, and RPA RTOG against the imaging models, a multivariate analysis was performed with age, RTOG RPA, PRM_{ADC+} and PRM_{rCBV-} for assessing one-year survival. Both age and RTOG RPA classification were not found to contribute to the statistical model.

Stratification of the patient population by each of the four models used, which includes RR, are presented as Kaplan-Meier plots in Figure 2. The median survivals for non-responders and responders as determined by PRM_{ADC+} were 8.3 months (95% confidence interval (CI): 6.2-10.4; $n=25$) and not reached ($n=20$), respectively. Using PRM_{rCBV-} to categorize non-responders and responders, their median survival was found to be 7.1 months (95% CI: 5.1-9.1; $n=22$) and 20.4 months (95% CI: 1.7-39.1; $n=23$), respectively. Median survivals for non-responders and responders as determined by RR were 8.1 months (95% CI: 6.0-10.2; $n=19$) and not reached ($n=26$), respectively. For the composite PRM model with the three discrete response groups median survivals for non-responders, intermediate and responders were 5.5 months (95% CI: 4.4-6.6 months $n=14$), 16 months (8.6-23.4 months $n=19$) and not reached ($n=12$), respectively. Using a log-rank test to assess significance, all four models were highly predictive of overall survival (Table 2). Performing this same statistical test pair-wise between response groups defined by the composite model found that non-responders had a significantly shorter survival than the intermediate and responder subpopulations ($p<0.0001$). Although not found to be significant based on our statistical criteria ($p<0.05$), the survival of responders when compared to intermediate generated a p value of 0.06. This is partly attributed to the small numbers analyzed in this study. Assessment of overall survival of all models in a unified multivariate test found PRM_{ADC+/PRM_{rCBV-}} assessed at week 3 mid-treatment to have the strongest statistical power even over RR.

In the cohort of patients studied, eight were diagnosed with grade 3 gliomas. Additional analysis was performed to determine if inclusion of these patients adversely affected the results presented above. As observed in Table 1, 7 of these patients had survived longer than one year with only a single patient surviving less than a year (OS was 5.1 months). This lone patient had a tumor that exhibited PRM values of ADC and rCBV indicative of a tumor non-responsive to therapy. Based on these results, the composite PRM categorized this patient as a non-responder. In fact, out of the 8 patients with grade 3 glioma, the composite model of PRM only identified the referenced patient as a non-responder, 3 were intermediate (mean OS (SD) was 22 (6.7) months) and 4 were responders (mean OS (SD) was 35 (19) months).

Finally, assessment of the composite PRM model when limited to grade 4 gliomas found the composite PRM to be significant for OS ($p < 0.0001$) with median survivals of 6 months ($n=13$) for non-responders, 12.8 months ($n=16$) for intermediate response, and median survival not reached at greater than 30 months in the 8 patients scored as responsive. Multivariate analyses, analogous to those performed in Table 2, of patients with grade 4 gliomas ($n=37$) identified a strong correlation of PRM_{ADC+}/PRM_{rCBV-} and RR to 6 month PFS ($p=0.016$ and $p=0.02$, respectively) and only PRM_{ADC+}/PRM_{rCBV-} to both one year survival ($p=0.002$) and overall survival ($p < 0.0001$).

Discussion

Personalized medicine in cancer care is slowly becoming a reality from the “one-size fits all” approach. Advances in molecular and histological biomarkers are now providing detailed information on tumor biology that is being used to individualize therapy (34). Pretreatment assessment using molecular and histological biomarkers is increasingly being used to dictate initial choice of therapy. There is also a critical need for the deployment of surrogate biomarkers of response to provide real-time information on the state of the tumor mid-treatment. With respect to assessment of treatment in GBM patients, modern advancements in neuroimaging techniques, such as MRI, positron emission tomography (PET), single photon emission computed tomography (SPECT) and computed tomography (CT), are providing detailed functional and quantitative information on tumor heterogeneity. More specifically, techniques utilizing MRI, with its high tissue contrast and resolution, are capable of imaging with high sensitivity changes in tumor microenvironment and hemodynamics at the cellular level allowing for early serial assessment of a tumor during treatment.

Standard management of malignant high grade gliomas continues to be concurrent temozolomide and radiation 60 Gy followed by adjuvant TMZ. Currently, randomized phase III studies are being conducted to determine the additional benefit of novel targeted therapies, including various signal transduction inhibitors encompassing monoclonal antibodies, e.g. Avastin (bevacizumab), as well as small molecules. However, these therapies are unlikely to benefit all patients and are extremely costly and associated with a significant increase in the risk of toxicity. Reliable predictive imaging biomarkers of response are important in selecting those patients most likely to benefit from alternative treatment strategies and selecting those patients as early as possible.

We and others have found quantitative neuroimaging methods are highly sensitive to analyzing treatment-induced cellularity and hemodynamic alterations within the tumor. Difficulties in analyzing these parametric maps ensue from the high spatial heterogeneity typical of gliomas. By focusing on regions of increasing or decreasing parameter value, the functional behavior of the tumor can be spatially dissected and interpreted for its prognostic value. Our group has demonstrated the improved prognostic capabilities of quantitative imaging techniques (DW- and DSC-MRI) when analyzed by PRM, which has been compared to standard histogram-based methods and radiological response (30, 33). Expanding further, we have demonstrated in the present study that a composite of ADC and rCBV as analyzed by PRM enhances the sensitivity of the biomarker for predicting those patients resistant to chemoradiation at 3 weeks post-treatment initiation.

It is important to note that administration of steroid would have no confounding effect on the results reported in this study. As indicated in the manuscript steroid doses were closely followed prior to treatment, weekly during radiation therapy, and at the time of each MRI (pre-treatment and 3 weeks during treatment). Given the close timing between the pre-treatment scan (within 5 days prior to the start of treatment) and the 3 week scan (on average

<21 days from the start of treatment) there were minimal to no changes in steroid dosing over this short time period. It has been our standard clinical practice not to taper steroids during the first several weeks of radiation therapy due to concerns for possible increased edema during the early course of therapy. Therefore, steroid doses were typically not adjusted until weeks 3-6 of radiation therapy. Further, the benefit seen by composite PRM was not simply a measure of generalized steroid effect since previous results have shown that the percentage change in either ADC and rCBV would also have been impacted by steroid dosing and were not prognostic (30, 33).

Varying MRI field strengths as well as Gd-DTPA doses used in DSC-MRI for calculating CBV were also not suspected of affecting the current results. It is important to note that ADC is independent of field strength. Nevertheless, from the total population studied (n=45), 31 were imaged at 1.5T and the remaining 14 were imaged at 3T. To avoid variability between scanners, the same scanner was used for a given patient throughout the study. An additional analysis was performed to determine if there were any systematic differences in mean ADC and rCBV values pre-therapy and at week 3 mid-treatment as well as differences in PRM_{ADC+} and PRM_{rCBV-} as a result of field strength using an unpaired Student's t-test. No significant differences in imaging parameters were observed as a result of field strength. As for varying dosing of contrast agent, our algorithm for calculating CBV mitigates the effects of variable Gd-DTPA dose by use of the arterial input function measured on each patient individually, which implicitly scales with the same dose factor. All our CBV analyses use values normalized by white matter CBV which further reduces dose dependency. To mitigate leakage bias as a result of T1 effects, we employed a pre-injection of contrast agent prior to a second bolus given during dynamic T2* imaging. In addition, we used a relatively long TR of 1.5-2 seconds to further reduce T1-weighting.

This is the first study that describes a composite model of PRM_{ADC+} and PRM_{rCBV-} obtained at week 3 in assessing tumor response. Our data shows that the composite model is a much stronger predictive factor of overall survival compared to either metric alone. This composite metric provides a novel imaging biomarker that has significant implications for early stratification in clinical trials in high grade glioma as well as potentially other clinical sites. When included in a single multivariate statistical analysis, the composite of PRM_{ADC+} and PRM_{rCBV-} obtained at week 3 was found to be a much stronger predictor of overall survival than either metric alone, as well as 10 week radiological response. Use of the composite imaging biomarker not only provides a more early and sensitive method for identifying populations of responders and nonresponders but also allowed for the identification of a third patient subgroup that exhibited an intermediate response pattern not previously shown by conventional response criteria. Ongoing studies are elucidating the molecular determinants of response that differentiate tumors from each of these three response groups. Such information could ultimately facilitate the design of improved therapies for GBM patients identified in this manner.

A biomarker that allows for early identification of patients resistant to standard of care also provides an opportunity to reassess treatment options in a timelier manner compared to current clinical practice (35-37). For example, determination of responsiveness at week 3 into temozolomide with concomitant radiotherapy could allow patients resistant to standard of care to be given adjuvant treatment or be moved more quickly to an aggressive salvage regimen. To obtain further support for this approach, we recently initiated a clinical trial utilizing the composite imaging biomarker at week 3 following treatment initiation to select non-responding patients for further treatment intensification with bevacizumab and dose painting IMRT. While a multicenter trial to validate these findings is warranted, the results presented herein currently support a future paradigm shift in the current clinical management of GBM to a more individualized approach. In GBM, this would also provide

an opportunity to develop new trials designed to improve patient outcome by selecting patients likely to benefit from more aggressive or experimental treatment regimens.

Materials and Methods

Patient Population

Patients newly diagnosed with histological confirmed grade III and IV gliomas were enrolled on a protocol of intra-treatment MRI. This cohort of patients has been used previously in published work investigating the prognostic value of PRM applied to the individual parameters ADC and rCBV (30, 33). Surgical resection was performed on all patients and the extent was evaluated by post-operative MRI obtained within 72 hours of resection. Radiotherapy was delivered using 3D-conformal therapy or intensity modulated radiation therapy. Standard techniques were utilized with a 2.0-2.5 cm margin on either the enhancing region on gadolinium-enhanced scans or the abnormal signal on T2-weighted scans to 46-50 Gy with the central gross tumor treated to a final median dose of 70 Gy in 6-7 weeks (38). Twenty-three of these individuals were treated on a phase 2 protocol of high-dose (>60 Gy) radiation therapy concurrent with temozolomide 75 mg/m² daily followed by adjuvant temozolomide 150-200 mg/m² daily for 5 days of a 28 day cycle. Remaining patients received radiation alone (n=22). Chemotherapy was commonly administered in both groups depending upon clinical circumstances (Table 1). None of these patients, accrued from 2000-2006, received any anti-angiogenic therapy during their primary treatment although some patients did receive Avastin at time of progression. Informed consent was obtained, and images and medical record use was approved by the University of Michigan Institutional Review Board.

MRI Examination

Patients were evaluated pre-therapy, three and 10 weeks after the start of radiation with follow-up scans every 2 to 3 months. DW- and DSC-MRI as well as standard MRI (fluid attenuation inversion recovery, T2-weighted and gadolinium-enhanced T1-weighted MRI) were performed on either a 1.5T Signa (General Electric Medical Systems) (n=31 subjects) or 3T Achieva (Philips Medical Systems) (n=14 subjects) system. Radiological response at 10 weeks was based on changes in tumor volume on T1-weighted contrast-enhanced MRI and steroid doses and was classified as complete response (CR), partial response (PR), stable disease (SD) and progressive disease (PD)(2). Steroid doses were recorded before each scan, weekly during radiotherapy, and at each follow-up (39).

Quantitative MRI

DW-MRI utilized a single-shot, spin-echo, diffusion-sensitized, echo-planar imaging (EPI) acquisition sequence. On the 1.5T system, 24 6-mm axial-oblique sections were acquired using a 22 cm-field of view (FOV) and 128 matrix with “b-factor” = 0 and 1000 s/mm² along three orthogonal directions (repetition time (TR) = 1000ms; echo time (TE) = 71 to 100 ms, and number of averages (NS) = 1). On the 3T system, at least 28 4-mm axial-oblique sections were acquired through the brain using a 24-cm FOV and 128 matrix (TR = 2636 ms; TE = 46ms; NS=1 for b=0, and NS=2 for b=1000 s/mm²). Parallel imaging (sensitivity encoding factor = 3) was used on 3T to reduce spatial distortion. The diffusion weighted images for the three orthogonal directions were used to calculate an apparent diffusion coefficient (ADC) map (33).

For DSC-MRI, 14 to 20 slices were acquired by a gradient-echo echo-planar imaging pulse sequence (TR=1.5 to 2s, TE=50 to 60ms, field of view 220×220 mm², matrix 128×128, flip angle 60°, and 4 to 6mm thickness and 0mm gap). Gadolinium-diethylenetriamine pentaacetic acid (Gd-DTPA; Bayer HealthCare Pharmaceuticals) was injected intravenously

with a dose of 0.05 to 0.1 ml kg⁻¹ as a bolus using a power injector at a rate of 2 mL s⁻¹, followed immediately by 15 cc of saline flush at the same rate. Subsequently a Gd-enhanced T₁-weighted imaging was acquired. Cerebral blood volume (CBV) map was generated from DSC images as described previously (40). To assess differences in tumor blood volume during chemoradiation therapy (cRT) and between subjects, CBV maps were normalized to values within white matter regions contralateral to the tumor to generate relative CBV maps (rCBV). For simplicity in notation, relative blood volumes for both *brain* and *tumor* have been denoted by “rCBV” throughout this article. The following guidelines were used to define the white matter regions of interest for normalization: (1) contralateral to tumor, (2) received <30 Gy accumulated dose, and 3) as large as possible but avoiding regions with susceptibility artifacts and partial volume averaging.

Image Analysis

Pre- and 3 week mid-treatment ADC and rCBV maps were co-registered to Gd-enhanced T₁-weighted images acquired before cRT using mutual information as an objective function and simplex as an optimizer (41). The co-registration of different and similar weighted MRI scans for the same subject is totally automatic and assumes a rigid-body geometry relationship, i.e. rotation and translation, between head scans. Following co-registration, brain tumors, manually contoured by a neuroradiologist, were defined within the enhancing regions of the tumor on the Gd-enhanced T₁-weighted images. Only patients with contrast-enhancing tumors ≥ 4cc were included in this study. For simplicity, tumor will refer to only the contrast-enhancing volume on a T₁-weighted post-contrast image. Shrinkage or growth of the tumor during the time between scans may have occurred; therefore, only voxels that are contrast enhancing on both the pre-RT and mid-RT tumor volumes were included. Subsequent to co-registration, the resultant maps consist of spatially aligned voxels with ADC and rCBV values prior and 3 weeks following treatment initiation.

The Parametric Response Map of any parameter (PRM_X, where X denotes any parametric map such as ADC and rCBV) was determined by first calculating the difference between X ($\Delta X = \text{mid } X - \text{baseline } X$) for each voxel within the tumor pre-therapy and at week 3 post-treatment initiation. Voxels yielding ΔX greater than a predetermined threshold (set to 1.2 and 55 for rCBV and ADC, respectively; details described previously (22, 30, 33)), were designated red (i.e. $\Delta rCBV > 1.2$; $\Delta ADC > 55$). Blue voxels represent volumes whose parameter value decreased by more than the threshold (i.e. $\Delta rCBV < -1.2$; $\Delta ADC < -55$) and the green voxels represent voxels within the tumor that were unchanged (i.e. $|\Delta rCBV| \leq 1.2$; $|\Delta ADC| \leq 5.5$). The volume fractions within the tumor determined from PRM_X were PRM_{X+} for increasing X, PRM_{X-} for decreasing X, and PRM_{X0} for unchanged X.

Data and Statistical Analyses

The patient population was stratified based on previously reported cutoff values of 4.7% and 6.8% for PRM_{ADC} and PRM_{rCBV}, respectively (30, 33). The composite model of these two dichotomized metrics was determined by categorizing patients as responders, non-responders or intermediate. Patients were designated non-responding if both single metrics predict non-responding (PRM_{ADC+} < 4.7% and PRM_{rCBV-} > 6.8%), whereas patients were designated responders when both single metrics predict responder (PRM_{ADC+} ≥ 4.7% and PRM_{rCBV-} ≤ 6.8%). For the cases where single metrics were in disagreement patients were designated intermediate (PRM_{ADC+} ≥ 4.7% and PRM_{rCBV-} > 6.8% or PRM_{ADC+} < 4.7% and PRM_{rCBV-} ≤ 6.8%). A univariate and multivariate logistic regression with forward entry was used to assess the predictive value of each metric for 6 month progression free survival (PFS) and one-year survival. Assessment of overall survival for the metrics was determined using a Kaplan-Meier analysis with log-rank test and a multivariate Cox regression with forward entry. Secondary analysis was performed to assess the predictive value of patient

characteristics to one year survival using either an unpaired Student's t-test or likelihood ratio test. All statistical computations were performed with a statistical software package (SPSS Software Products), and results were declared statistically significant at the two-sided 5% comparison-wise significance level ($p < 0.05$).

Acknowledgments

Grant Support: NIH grants P01CA85878, P50CA93990 and P01CA087634. The costs of publication of this article were defrayed in part by the payment of page charges. This article must therefore be hereby marked advertisement in accordance with 18 U.S.C. Section 1734 solely to indicate this fact.

Funding: This work was supported by the US National Institutes of Health research grants P01CA085878, P01CA087634 and P50CA093990.

References

1. Stupp R, Hegi ME, Mason WP, van den Bent MJ, Taphoorn MJ, Janzer RC, et al. Effects of radiotherapy with concomitant and adjuvant temozolomide versus radiotherapy alone on survival in glioblastoma in a randomised phase III study: 5-year analysis of the EORTC-NCIC trial. *Lancet Oncol.* 2009; 10:459–66. [PubMed: 19269895]
2. Macdonald DR, Cascino TL, Schold SC Jr, Cairncross JG. Response criteria for phase II studies of supratentorial malignant glioma. *J Clin Oncol.* 1990; 8:1277–80. [PubMed: 2358840]
3. Stupp R, Mason WP, van den Bent MJ, Weller M, Fisher B, Taphoorn MJ, et al. Radiotherapy plus concomitant and adjuvant temozolomide for glioblastoma. *N Engl J Med.* 2005; 352:987–96. [PubMed: 15758009]
4. Wen PY, Macdonald DR, Reardon DA, Cloughesy TF, Sorensen AG, Galanis E, et al. Updated response assessment criteria for high-grade gliomas: response assessment in neuro-oncology working group. *J Clin Oncol.* 2010; 28:1963–72. [PubMed: 20231676]
5. Stupp R, Hegi ME, Neyns B, Goldbrunner R, Schlegel U, Clement PM, et al. Phase I/IIa study of cilengitide and temozolomide with concomitant radiotherapy followed by cilengitide and temozolomide maintenance therapy in patients with newly diagnosed glioblastoma. *J Clin Oncol.* 2010; 28:2712–8. [PubMed: 20439646]
6. Harry VN, Semple SI, Parkin DE, Gilbert FJ. Use of new imaging techniques to predict tumour response to therapy. *Lancet Oncol.* 2010; 11:92–102. [PubMed: 20129132]
7. Chenevert TL, Ross BD. Diffusion imaging for therapy response assessment of brain tumor. *Neuroimaging Clin N Am.* 2009; 19:559–71. [PubMed: 19959005]
8. Lacerda S, Law M. Magnetic resonance perfusion and permeability imaging in brain tumors. *Neuroimaging Clin N Am.* 2009; 19:527–57. [PubMed: 19959004]
9. Chenevert TL, Stegman LD, Taylor JM, Robertson PL, Greenberg HS, Rehemtulla A, et al. Diffusion magnetic resonance imaging: an early surrogate marker of therapeutic efficacy in brain tumors. *J Natl Cancer Inst.* 2000; 92:2029–36. [PubMed: 11121466]
10. Hamstra DA, Lee KC, Moffat BA, Chenevert TL, Rehemtulla A, Ross BD. Diffusion magnetic resonance imaging: an imaging treatment response biomarker to chemoradiotherapy in a mouse model of squamous cell cancer of the head and neck. *Transl Oncol.* 2008; 1:187–94. [PubMed: 19043529]
11. Liimatainen T, Hakumaki JM, Kauppinen RA, Ala-Korpela M. Monitoring of gliomas in vivo by diffusion MRI and (1)H MRS during gene therapy-induced apoptosis: interrelationships between water diffusion and mobile lipids. *NMR Biomed.* 2009; 22:272–9. [PubMed: 19009568]
12. Liu Y, Bai R, Sun H, Liu H, Zhao X, Li Y. Diffusion-weighted imaging in predicting and monitoring the response of uterine cervical cancer to combined chemoradiation. *Clin Radiol.* 2009; 64:1067–74. [PubMed: 19822239]
13. Brix G, Kiessling F, Lucht R, Darai S, Wasser K, Delorme S, et al. Microcirculation and microvasculature in breast tumors: pharmacokinetic analysis of dynamic MR image series. *Magn Reson Med.* 2004; 52:420–9. [PubMed: 15282828]

14. Ostergaard L, Sorensen AG, Kwong KK, Weisskoff RM, Gyldensted C, Rosen BR. High resolution measurement of cerebral blood flow using intravascular tracer bolus passages. Part II: Experimental comparison and preliminary results. *Magn Reson Med.* 1996; 36:726–36. [PubMed: 8916023]
15. Ostergaard L, Weisskoff RM, Chesler DA, Gyldensted C, Rosen BR. High resolution measurement of cerebral blood flow using intravascular tracer bolus passages. Part I: Mathematical approach and statistical analysis. *Magn Reson Med.* 1996; 36:715–25. [PubMed: 8916022]
16. Rosen BR, Belliveau JW, Vevea JM, Brady TJ. Perfusion imaging with NMR contrast agents. *Magn Reson Med.* 1990; 14:249–65. [PubMed: 2345506]
17. Tofts PS. Modeling tracer kinetics in dynamic Gd-DTPA MR imaging. *J Magn Reson Imaging.* 1997; 7:91–101. [PubMed: 9039598]
18. Degani H, Gusic V, Weinstein D, Fields S, Strano S. Mapping pathophysiological features of breast tumors by MRI at high spatial resolution. *Nat Med.* 1997; 3:780–2. [PubMed: 9212107]
19. Hu LS, Baxter LC, Smith KA, Feuerstein BG, Karis JP, Eschbacher JM, et al. Relative cerebral blood volume values to differentiate high-grade glioma recurrence from posttreatment radiation effect: direct correlation between image-guided tissue histopathology and localized dynamic susceptibility-weighted contrast-enhanced perfusion MR imaging measurements. *AJNR Am J Neuroradiol.* 2009; 30:552–8. [PubMed: 19056837]
20. Law M, Oh S, Johnson G, Babb JS, Zagzag D, Golfinos J, et al. Perfusion magnetic resonance imaging predicts patient outcome as an adjunct to histopathology: a second reference standard in the surgical and nonsurgical treatment of low-grade gliomas. *Neurosurgery.* 2006; 58:1099–107. discussion -107. [PubMed: 16723889]
21. Law M, Yang S, Wang H, Babb JS, Johnson G, Cha S, et al. Glioma grading: sensitivity, specificity, and predictive values of perfusion MR imaging and proton MR spectroscopic imaging compared with conventional MR imaging. *AJNR Am J Neuroradiol.* 2003; 24:1989–98. [PubMed: 14625221]
22. Moffat BA, Chenevert TL, Lawrence TS, Meyer CR, Johnson TD, Dong Q, et al. Functional diffusion map: a noninvasive MRI biomarker for early stratification of clinical brain tumor response. *Proc Natl Acad Sci U S A.* 2005; 102:5524–9. [PubMed: 15805192]
23. Ellingson BM, Malkin MG, Rand SD, Connelly JM, Quinsey C, LaViolette PS, et al. Validation of functional diffusion maps (fDMs) as a biomarker for human glioma cellularity. *J Magn Reson Imaging.* 2010; 31:538–48. [PubMed: 20187195]
24. Hiramatsu R, Kawabata S, Miyatake SI, Yamada Y, Kuroiwa T. An Imaging Assessment of Malignant Glioma Patients Treated by Boron Neutron Capture Therapy Using Functional Diffusion Map. *Neuro-Oncology.* 2009; 11:669.
25. Lin YC, Wang CC, Wai YY, Wan YL, Ng SH, Chen YL, et al. Significant temporal evolution of diffusion anisotropy for evaluating early response to radiosurgery in patients with vestibular schwannoma: findings from functional diffusion maps. *AJNR Am J Neuroradiol.* 2010; 31:269–74. [PubMed: 19779002]
26. Ellingson BM, Rand SD, Malkin MG, Schmainda KM. Utility of functional diffusion maps to monitor a patient diagnosed with gliomatosis cerebri. *J Neurooncol.* 2009
27. Galban CJ, Mukherji SK, Chenevert TL, Meyer CR, Hamstra DA, Bland PH, et al. A feasibility study of parametric response map analysis of diffusion-weighted magnetic resonance imaging scans of head and neck cancer patients for providing early detection of therapeutic efficacy. *Transl Oncol.* 2009; 2:184–90. [PubMed: 19701503]
28. Lee KC, Bradley DA, Hussain M, Meyer CR, Chenevert TL, Jacobson JA, et al. A feasibility study evaluating the functional diffusion map as a predictive imaging biomarker for detection of treatment response in a patient with metastatic prostate cancer to the bone. *Neoplasia.* 2007; 9:1003–11. [PubMed: 18084607]
29. Ma B, Meyer CR, Pickles MD, Chenevert TL, Bland PH, Galban CJ, et al. Voxel-by-voxel functional diffusion mapping for early evaluation of breast cancer treatment. *Inf Process Med Imaging.* 2009; 21:276–87. [PubMed: 19694270]

30. Galban CJ, Chenevert TL, Meyer CR, Tsien C, Lawrence TS, Hamstra DA, et al. The parametric response map is an imaging biomarker for early cancer treatment outcome. *Nat Med.* 2009; 15:572–6. [PubMed: 19377487]
31. Tsien C, Galban CJ, Chenevert TL, Johnson TD, Hamstra DA, Sundgren PC, et al. Parametric response map as an imaging biomarker to distinguish progression from pseudoprogression in high-grade glioma. *J Clin Oncol.* 2010; 28:2293–9. [PubMed: 20368564]
32. Curran WJ Jr, Scott CB, Horton J, Nelson JS, Weinstein AS, Fischbach AJ, et al. Recursive partitioning analysis of prognostic factors in three Radiation Therapy Oncology Group malignant glioma trials. *J Natl Cancer Inst.* 1993; 85:704–10. [PubMed: 8478956]
33. Hamstra DA, Galban CJ, Meyer CR, Johnson TD, Sundgren PC, Tsien C, et al. Functional diffusion map as an early imaging biomarker for high-grade glioma: correlation with conventional radiologic response and overall survival. *J Clin Oncol.* 2008; 26:3387–94. [PubMed: 18541899]
34. Sulman EP, Guerrero M, Aldape K. Beyond grade: molecular pathology of malignant gliomas. *Semin Radiat Oncol.* 2009; 19:142–9. [PubMed: 19464628]
35. Potti A, Schilsky RL, Nevins JR. Refocusing the war on cancer: the critical role of personalized treatment. *Sci Transl Med.* 2010; 2:28cm13.
36. Schilsky RL. How not to treat cancer. *Lancet Oncol.* 2008; 9:504–5. [PubMed: 18510981]
37. Schilsky RL. Personalized medicine in oncology: the future is now. *Nat Rev Drug Discov.* 2010; 9:363–6. [PubMed: 20431568]
38. Chan JL, Lee SW, Fraass BA, Normolle DP, Greenberg HS, Junck LR, et al. Survival and failure patterns of high-grade gliomas after three-dimensional conformal radiotherapy. *J Clin Oncol.* 2002; 20:1635–42. [PubMed: 11896114]
39. Levin VA, Crafts DC, Norman DM, Hoffer PB, Spire JP, Wilson CB. Criteria for evaluating patients undergoing chemotherapy for malignant brain tumors. *J Neurosurg.* 1977; 47:329–35. [PubMed: 894339]
40. Cao Y, Tsien CI, Nagesh V, Junck L, Ten Haken R, Ross BD, et al. Survival prediction in high-grade gliomas by MRI perfusion before and during early stage of RT [corrected]. *Int J Radiat Oncol Biol Phys.* 2006; 64:876–85. [PubMed: 16298499]
41. Meyer CR, Boes JL, Kim B, Bland PH, Zasadny KR, Kison PV, et al. Demonstration of accuracy and clinical versatility of mutual information for automatic multimodality image fusion using affine and thin-plate spline warped geometric deformations. *Med Image Anal.* 1997; 1:195–206. [PubMed: 9873906]

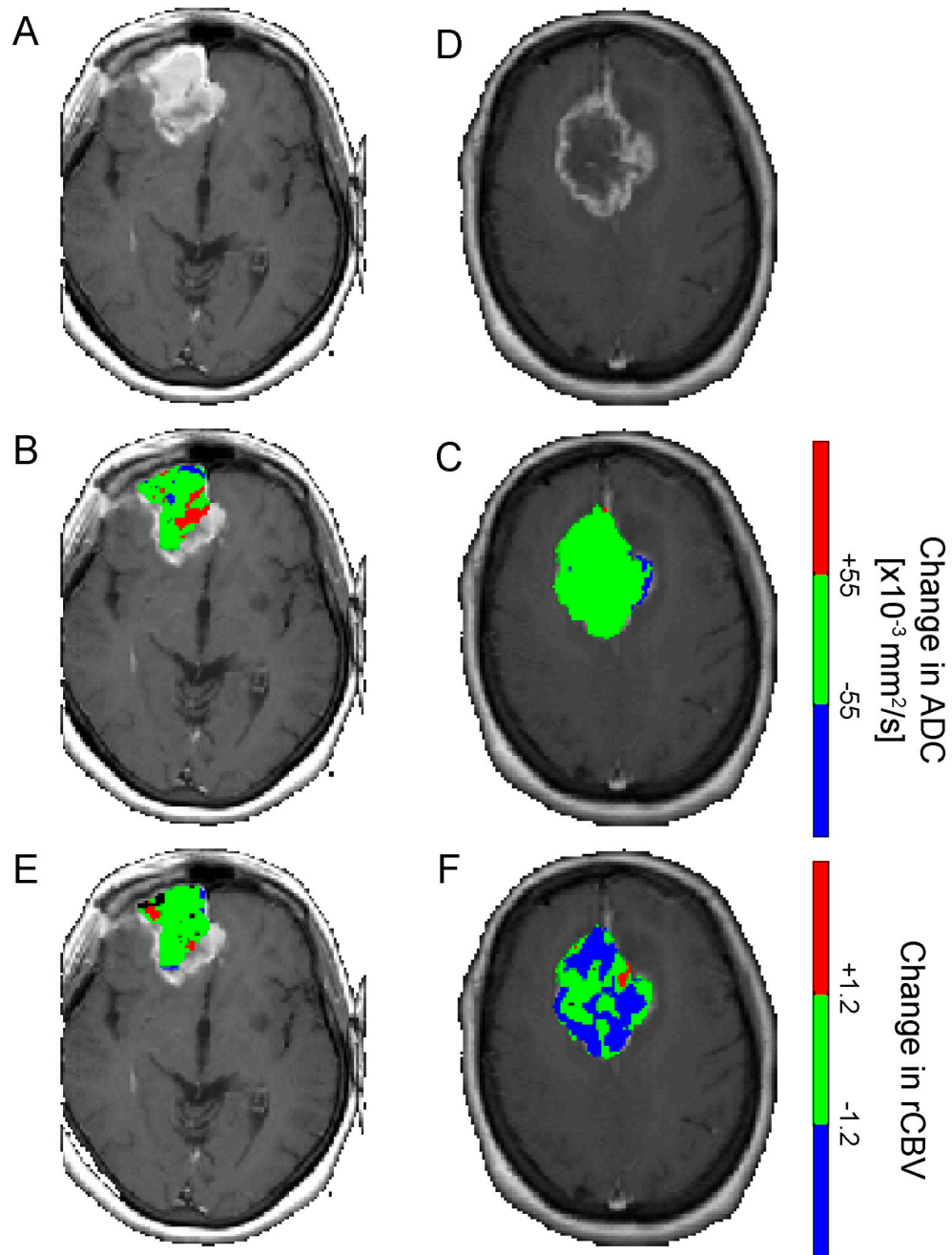


Figure 1. Representative (A,D) contrast-enhanced images and PRM overlays applied to (B,E) ADC and (C,F) rCBV from a (A-C) responding and (D-E) non-responding patients. The responding patient, diagnosed with a glioblastoma, had an overall survival of 17 months, $\text{PRM}_{\text{ADC}^+}$ of 12% and $\text{PRM}_{\text{rCBV}^-}$ of 4%. In contrast, the non-responding subject, also diagnosed with a glioblastoma, had an overall survival of 2 months, $\text{PRM}_{\text{ADC}^+}$ of 1% and $\text{PRM}_{\text{rCBV}^-}$ of 40%. PRM was acquired using pretreatment and 3 week post-treatment initiation imaging data.

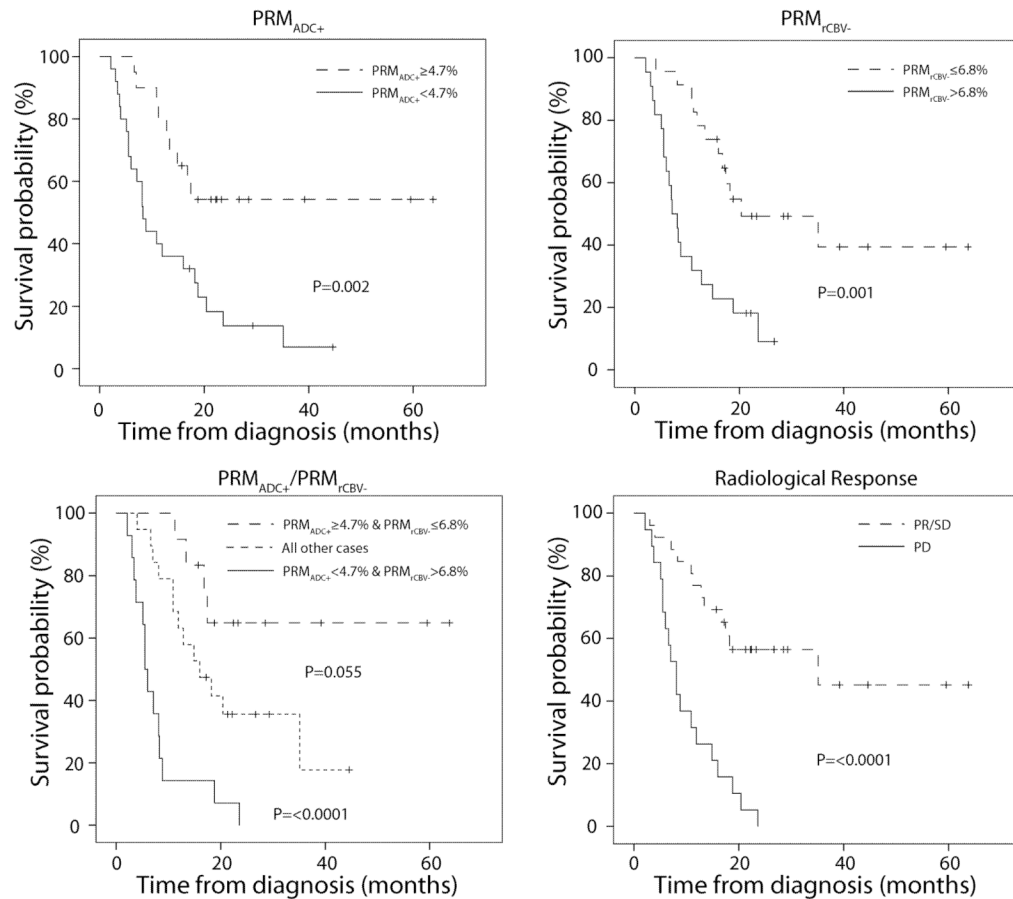


Figure 2.

Kaplan-Meier survival plots for overall survival, presented as a function of (a) PRM_{ADC+} , (b) PRM_{rCBV-} and (c) PRM_{ADC+}/PRM_{rCBV-} stratification at week 3 post-treatment initiation and (d) Radiological Response stratification at week 10 post-treatment initiation. The three discrete groups, as categorized by the composite PRM model, had median survivals for non-responders, intermediate and responders of 5.5 months (95% CI: 4.4-6.6 months n=14), 16 months (8.6-23.4 months n=19) and not reached (n=12), respectively.

Table 1
Patient characteristics

Variable		<1 year survival	≥1 year survival	p values
Total		20	25	
Age	(years)	60.9±2.4	48.6±3.1	0.003*
Pre-treatment Tumor volume	CE-T1 (cm ³)	45.1 ±8.1	31.9±4.7	0.166
Pre-treatment Tumor volume	FLAIR (cm ³)	103.9±11.6	92.0±16.8	0.566
Pathology	Grade 3	1	7	0.059#
	Grade 4	19	18	
Karnofsky performance status	<70	8	5	0.141#
	70+	12	20	
Location	Frontal/Temporal	12	18	0.397#
	Other	8	7	
Surgery	Biopsy	10	6	0.191#
	Sub-total	5	10	
	Near GTR	5	9	
Recursive partition analysis	1	0	3	0.025#
	2	0	0	
	3	3	7	
	4	5	8	
	5	5	6	
	6	7	1	
Radiation Therapy	Dose (Gy)	68.2±2.0	70.4±1.4	0.375*
MacDonald Criteria	PR/SD	6	20	0.001#
	PD	14	5	

Note: Statistical significance were assessed at $p < 0.05$ using an unpaired Student's t-test (*) and Likelihood Ratio (#). Pre-treatment tumor volumes were determined on contrast-enhanced T1 weighted images (CE-T1) and FLAIR images.

Table 2

Statistical analyses of parametric models

Model	6 month PFS		One Year Survival		Overall Survival	
	Univariate p values	Multivariate p values	Univariate p values	Multivariate p values	Univariate p values	Multivariate p values
PRM _{ADC+}	0.021		0.003		0.002	
PRM _{CBV-}	0.001		0.001		0.001	
PRM _{ADC+/PRM_{IGI}BV-}	<0.0001	0.012	<0.0001	<0.0001	<0.0001	<0.0001
Radiological Response	<0.0001	0.005	0.001		<0.0001	

Note: All parameter models were assessed at 6 month progression free survival (PFS), one year survival and overall survival. The Likelihood ratio test from a univariate and multivariate logistic regressions was used to determine a significant fit of parametric models to 6 month PFS or one year survival. The log-rank test was used to assess correlation of individual models to overall survival. Multivariate Cox regression was performed on all parametric models presented to determine the correlation of respective models to overall survival. All multivariate analyses were performed using a forward entry algorithm. Statistical significance was assessed at $p < 0.05$.